THE JOURNAL OF PHYSICAL CHEMISTRY C

Article

pubs.acs.org/JPCC

Ice-like Water Structure in Carbon Nanotube (8,8) Induces Cationic Hydration Enhancement

Zhongjin He,[†,‡] Jian Zhou,[*,†] Xiaohua Lu,[§] and Ben Corry[*,‡]

[†]School of Chemistry and Chemical Engineering, South China University of Technology, Guangzhou, Guangdong 510640, China

[§]State Key Laboratory of Materials-oriented Chemical Engineering, Nanjing University of Technology, Nanjing 210009, China

[‡]Research School of Biology, The Australian National University, Canberra ACT 0200, Australia

Supporting Information

ABSTRACT: It is well recognized that ice-like water can be formed in carbon nanotubes (CNTs). Here, we perform molecular dynamics simulations of the hydration of Na^+, K^+ and Cl^- in armchair CNT(n,n) (n = 6, 7, 8, 9 and 10) at 300 K to elucidate the effect of such water structures on ionic hydration. It is found that the interaction of Na^+ and K^+ with the water molecules is enhanced in CNT(8,8), but is similar or weaker than in bulk in the other CNTs. In bulk, water molecules orient in specific directions around ions due to the electrostatic interaction between them. Under the confinement of CNTs, the hydrogen bonds formed in the first hydration shell of Na^+ and K^+ disturb this orientation greatly. An exception is in CNT(8,8), where the dipole orientation is even more favorable for cations than in bulk due to the formation of a unique ice-like water structure that aligns the water molecules in specific directions. In contrast, the coordination number is more important than hydration shell orientation in determining the Cl^-–water interaction. Additionally, the preference for ions to adopt specific radial positions in the CNTs also affects ionic hydration.

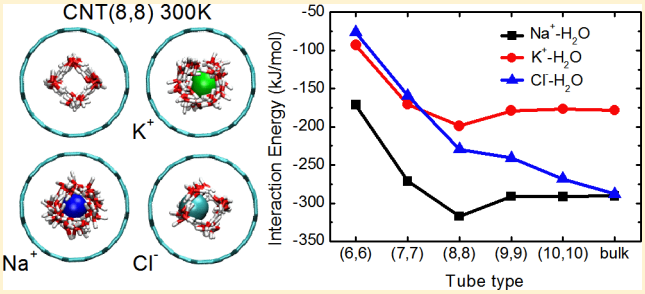

INTRODUCTION

The hydration of ions under nanoscale confinement has attracted much attention for its critical role in a wide range of technological applications and in dictating transport in biological ion channels. Recently, carbon nanotubes (CNTs) have been proposed to be used in the construction of novel nanofluidic systems, high-performance membranes, electrochemical capacitors and electrodes. These applications take advantage of the fast mass transport through the interior of the structure, the ease of chemical functionalization and the high surface area of CNTs.[1,2] Several CNT-based nanofluidic systems have been fabricated, which can be used as nanoscale flow sensors,[3] mass conveyors[4] and single ion detectors.[5] Pristine or modified CNTs with narrow diameter may be able to selectively transport water molecules while rejecting ions.[6] Therefore, narrow CNTs can be incorporated into reverse or forward osmosis membranes for efficient seawater desalination.[7−9] In addition, a series of ion-selective CNTs, which mimic the function of biological systems, were designed via molecular dynamics (MD) simulations,[10,11] and the hydration structure of ions confined in the CNTs is essential to the remarkable ion selectivity.[12] CNTs are found to have great potential in methanol–water separation for the high selective adsorption of methanol.[13,14]

The hydration of ions in the confines of biological ion channels is critical in dictating ion conduction and selectivity in narrow pores. For example, the different selectivity of potassium and sodium channels is at least partly due to differences in ion hydration. In the filter of K^+-selective channel KcsA, K^+ is almost totally dehydrated and better coordinated by carbonyl groups than Na^+.[15] The slightly modified NaK channel loses selectivity as ions can be hydrated by additional water molecules.[16] The selectivity of voltage gated sodium channels for Na^+ over K^+ is suggested to be dictated by the more favorable solvation structure of Na^+ confined in the charged pore.[17] Ion dehydration has also been proposed as playing an important role in channel gating, preventing the passage of ions in channels even when the pore is not completely occluded.[18] CNTs can be used as a simple model to investigate ionic hydration under nanoscale confinement, without the intrinsic complexity and flexibility of biological pores. A detailed understanding of ionic hydration in CNTs can help facilitate the development of novel CNT-based devices and may give insight into the mechanisms of ion permeation and selectivity taking place in biological ion channels.

Ion hydration under nanoscale confinement is quite different from that in bulk.[19−26] Previous MD simulation results show that ions are desolvated and can easily form ion pairs in narrow CNTs;[27,28] however, the first hydration shell of ions in wide CNTs is almost bulk-like, and its size does not change.[29,30] Ions

Received: March 13, 2013
Revised: April 27, 2013
Published: May 2, 2013

   dx.doi.org/10.1021/jp4025206 | J. Phys. Chem. C 2013, 117, 11412−11420

in the aqueous electrolyte solution confined in CNTs are found to preferentially reside near the solution-CNT interface, as revealed by MD simulations with polarizable force field and first-principles studies.[31,32] The transport of ions through CNTs and the effect of temperature on ion hydration in CNTs have also been explored theoretically.[33,34] The solvation numbers of Rb^+, Br^-, Zn^{2+} and other ions confined in slit-shaped carbon nanospace and carbon nanopores have been determined experimentally.[35−38] The results showed that ions were desolvated in narrow nanopores. Recently, Ohba and co-workers have investigated the structure of NaCl aqueous solution confined in the CNTs with an average diameter of 2 nm with synchrotron X-ray diffraction.[39] They found that the intermolecular distance of water in the confined solution was stretched and the hydrogen bonds were weakened. They speculated that this was caused by the enhanced hydration shell formation of ions. In order to understand the processes taking place in these narrow pores, the underlying mechanism that leads to hydrogen bond breakage and the atomic-level hydration structure of ions need further exploration. MD simulation may be the best method to address this issue effectively.

Despite many achievements, the understanding of ionic hydration under nanoscale confinement is far from complete. Many experimental and theoretical studies have been performed to investigate the effect of ionic hydration on the hydrogen-bonding and other properties of water in bulk solution.[40] However, how the hydrogen-bonding taking place between water molecules in bulk and under nanoscale confinement affects ionic hydration is still not clear. It has been widely recognized that hydrogen-bonding water networks in CNTs result in specific water structures at low temperature and even ambient conditions that are not found in bulk.[41−43] One important issue to address is the effect of the hydrogen bonded networks present in CNTs on the ability of water to hydrate ions. In addition, great emphasis was previously put on determining the nature of the first hydration shell of ions confined in CNTs, but other shells were rarely investigated. Therefore, how all the hydration shells will be affected by the nanoscale confinement and water hydrogen-bond structures in CNTs requires systematic study. Given that Na^+, K^+ and Cl^- are ubiquitous in chemical processes and the physiological environment, we perform MD simulations of the hydration of these ions in armchair CNTs of a range of sizes, CNT(n,n) (n = 6,7,8,9 and 10), to elucidate these issues.

COMPUTATION METHODS

The simulation model used in this study is shown in Figure 1. A CNT with length of 6.15 nm was embedded in the horizontal direction between two graphite sheets to form a membrane. Water reservoirs were attached at both sides of the membrane for their importance as highlighted by Chialvo and Cummings.[26] The size of the reservoir was 5.27 nm × 5.22 nm × 2.50 nm. Such models were constructed for CNT(6,6), -(7,7), -(8,8), -(9,9) and -(10,10), whose effective internal diameters, assuming a carbon atom van der Waals radius of 0.17 nm, were 0.474, 0.610, 0.746, 0.881 and 1.017 nm, respectively. The system contains a pair of Na^+ (or K^+) and Cl^- ions and 4623 to 4725 water molecules depending on the size of the CNT used in the model, i.e., approaching infinite dilution. The system was equilibrated for 1 ns before any subsequent simulations to obtain proper water density in the CNT.

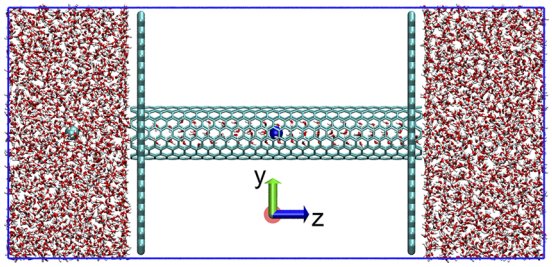

Figure 1. Snapshot of the simulation system. CNT and the two graphite sheets are in cyan. Water molecules are depicted as red and white rods. The blue and cyan balls represent Na^+ and Cl^-, respectively.

In each system, the ion studied was initially placed in the center of the CNT and allowed to move freely without any restraint. In order to avoid the formation of ion pairs, another ion carrying the opposite charge was fixed in the water reservoir to neutralize the system. The CNT and graphite sheets were held stationary. Periodic boundary conditions were applied in three dimensions. After energy minimization, each system was equilibrated for 100 ps. For data collection a 1 ns MD run was performed because ions can easily move out of CNTs in longer simulations. Coordinates were stored every 0.1 ps for analysis.

In the simulations, CNT carbon atoms were modeled as Lennard-Jones particles with the parameters of sp^2-like aromatic carbon in the AMBER03 force field.[44] SPC/E model[45] was used for water. The parameters for Na^+, K^+ and Cl^- were also taken from the AMBER03 force field. The cutoff distance for short-range van der Waals interactions was 1.0 nm. The long-range electrostatic interactions were computed by using a particle mesh Ewald (PME) method.[46] The settle algorithm[47] was used to constrain the geometry of water molecules. Trajectories were integrated using the leapfrog scheme with a time step of 2 fs. For comparison, the ionic hydration in bulk water (box size of 3.0 nm × 3.0 nm × 3.0 nm) was also simulated. Other simulation details were the same as those of the CNT system. For all the simulations, the NVT ensemble was implemented. The temperature was maintained at 300 K by using the Nosé−Hoover thermostat[48] with a time constant of 0.1 ps. All the simulations were performed using GROMACS4.5.4 software.[49] For each system, three independent MD simulations with different initial positions and velocities for water and ions were carried out. The average results and error bars of the three MD simulations were calculated. The error bars are not shown on the figures due to their small magnitude.

RESULTS AND DISCUSSION

Hydrogen-Bond Structures of Water Confined in CNTs. Specific structures of water in the CNTs are formed during the equilibration simulation, as shown in Figure 2A and reported previously.[42] A single-file water chain and two columns of water molecules exist in CNT(6,6) and -(7,7), respectively. In CNT(8,8), water molecules are close-packed into four columns with square-like structures. A hexagonal structure of water molecules is formed in CNT(9,9). In wide CNT(10,10), layers of water structures are formed near the tube wall with some less structured water molecules located at the tube axis. To depict these water structures in CNTs in more detail, φ is defined as the angle between the water dipole and the positive direction of the z-axis (CNT axis). Figure 2B

dx.doi.org/10.1021/jp4025206 | J. Phys. Chem. C 2013, 117, 11412−11420

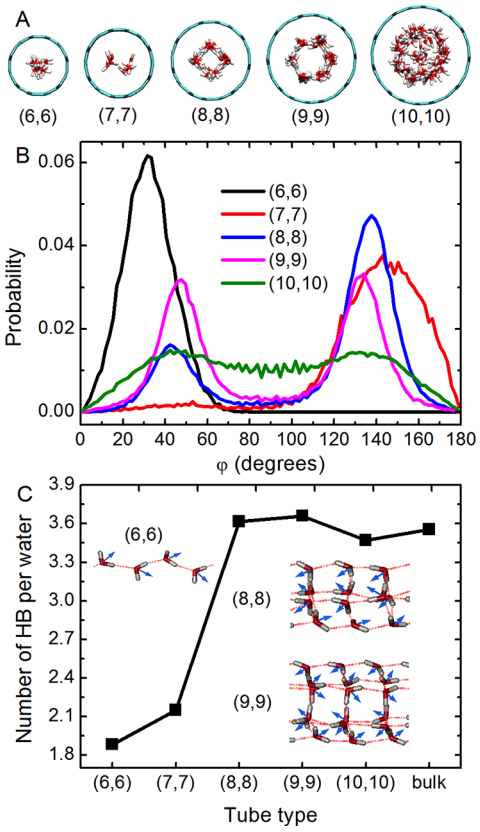

Figure 2. Water structures in CNTs. (A) Cross-sectional views of water inside CNTs. (B) Probability distributions of the dipole orientation of water molecules in each CNT; φ is the angle between a water dipole and the positive direction of the z-axis (CNT axis). (C) Average number of hydrogen bonds (HB) per water in CNTs and in bulk. The inset shows the water dipole (blue arrow) as well as hydrogen bonds (red dash lines) in three of the CNTs.

displays the distribution of φ averaged over all the water inside the CNT over the last 500 ps of the equilibration simulation. The sharp peak located at around 30° in CNT(6,6) and the wide peak located at about 140° in CNT(7,7) indicate that water dipoles prefer to point either way along the CNT axis in CNT(6,6) and CNT(7,7). In CNT(8,8), the height of the peak around 140° is about three times that of the peak around 40°. After inspecting the simulation trajectories, we find that the dipole of three columns of water molecules points to the left while the other column points right, as shown in the inset of Figure 2C. However, in the subsequent 30 ns MD simulation, the water structures in CNT(8,8) can adopt another two configurations: one column pointing to the left and the other three columns pointing to the right or two columns pointing to the left and the other two columns pointing to the right. The thermal fluctuation at 300 K could surmount the small energy barrier among these configurations and makes them transform into each other. Thus, the 4-gonal ice-like water formed in CNT(8,8) at room temperature shows ferroelectricity over some short periods of the simulation, but does not show when averaged over a long time period. Previous studies[50,51] found that even-number-gonal ice nanotubes formed in CNTs under low temperatures do not exhibit spontaneous polarizations while the odd-number-gonal ones do. In CNT(9,9), the dipole of three columns of water molecules points left while the other three columns point right. In addition, the direction of the dipole in one column is opposite to that of its two neighboring columns. Therefore, the two peaks in CNT(9,9) are of the same height, pictured in Figure 2B. Moreover, such water configuration in CNT(9,9) is very stable and maintained during the following 30 ns MD simulation. Hence, 6-gonal ice-like water formed in CNT(9,9) at room temperature is antiferroelectric, similar to the even-number-gonal ice nanotubes formed in CNTs under low temperatures.[50,51] However, water molecules in wide CNT(10,10) have no obvious dipole orientation preference.

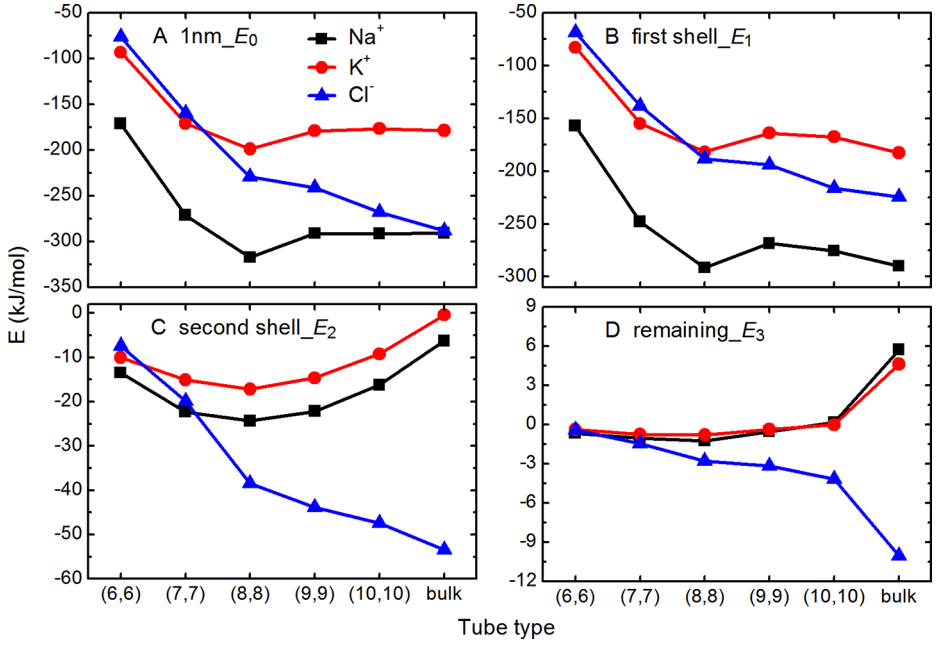

Figure 3. The interaction energy between ions and water molecules within (A) 1 nm (E_0), (B) the first shell (E_1), (C) the second shell of ions (E_2) and (D) in the remaining region (E_3) (that is beyond the second shell but within 1 nm of ions) in CNTs and bulk solution.

dx.doi.org/10.1021/jp4025206 | J. Phys. Chem. C 2013, 117, 11412−11420

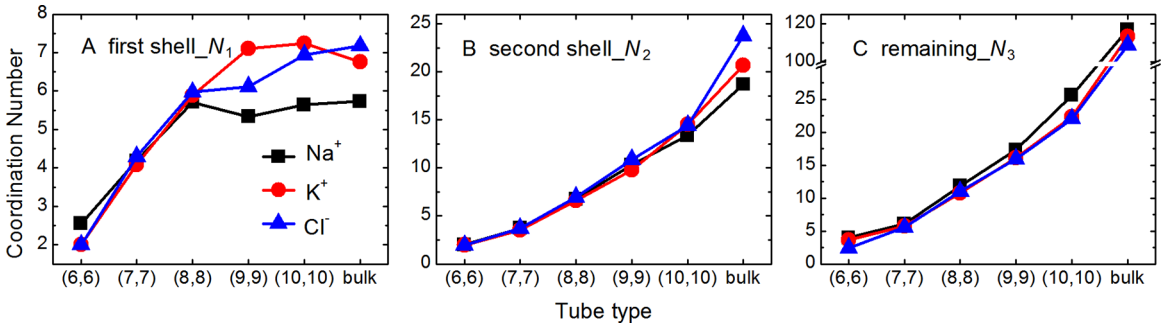

Figure 4. The coordination number of ions of (A) their first shell (N_1), (B) their second shell (N_2) and (C) the remaining region (N_3) (that is beyond the second shell but within 1 nm of ions) in CNTs and bulk solution.

Interestingly, these special water structures with specific dipole orientation preference can facilitate hydrogen-bond formation in CNTs. Figure 2C depicts the average number of hydrogen bonds per water in CNTs and in bulk. A hydrogen bond is identified when two oxygen atoms are closer than 3.5 Å and the angle ∠OHO is greater than 120°. With this definition, 3.55 hydrogen bonds per water molecule are obtained at ambient conditions, agreeing well with the experimental value 3.58.[52] The hydrogen bond number per water molecule is greatly lowered in narrow CNT(6,6) and -(7,7) due to the extreme confinement. In contrast, the mean number of hydrogen bonds per water is bulk-like in CNT(8,8), -(9,9) and -(10,10). It should be noted that the formation of such ice-like water structures at ambient conditions is independent of water model. Previous simulation studies with TIP3P, TIP4P-EW and TIP5P water models also found such a water phase.[7,53−55] Furthermore, recent experimental studies[56−58] confirmed these simulation findings. Such ice-like water in CNT(8,8) and -(9,9) has many anomalous properties, such as high viscosity[54] and low diffusibility,[42,59] and can affect ionic hydration in CNTs profoundly, as discussed below.

Interaction Energy between Ions and Water Molecules. The ion hydration properties in CNTs were first analyzed in terms of energy.[60] The interaction energy (E_0) between ions and the water molecules within 1 nm of each ion is plotted in Figure 3A. The E_0 for Na^+, K^+ and Cl^- are −290.6 ± 0.3, −178.5 ± 0.3 and −288.0 ± 0.2 kJ mol^{-1} in bulk solution, indicating that the ionic hydration strength for Na^+ is the strongest and K^+ weakest, which agrees well with other simulation results.[61,62] In narrower CNT(6,6) and -(7,7), the E_0 for Na^+ and K^+ is greatly weakened. However, an anomalous phenomenon occurs in CNT(8,8) for both cations. The E_0 values for Na^+ and K^+ are increased to −317.3 ± 1.0 and −199.0 ± 0.5 kJ mol^{-1}, respectively; 26.7 ± 1.0 and 20.5 ± 0.6 kJ mol^{-1} stronger than their bulk level. In wider CNT(9,9) and -(10,10), the E_0 values of both cations are bulk-like. In contrast with the situation for cations, the magnitude of E_0 of Cl^- increases monotonically to the bulk level with the diameter of the CNTs.

To figure out the origin of the anomalous interaction change between ions and water molecules in CNT(8,8), we decompose E_0 into the interaction energy between ions and water molecules within the first shell (E_1), second shell (E_2) and in the remaining region (that is beyond the second shell but within 1 nm of ions) (E_3). The interaction between both cations and water molecules in their first shells is weakened in all CNTs except in CNT(8,8), where the E_1 values of both cations are bulk-like, as shown in Figure 3B. Interestingly, Na^+ and K^+ interact with the water molecules in their second shells more strongly in all the CNTs than in bulk. The greatest difference in E_2 compared to bulk is again found in CNT(8,8), with statistically significant difference of 18.1 ± 0.3 and 16.8 ± 0.3 kJ mol^{-1} found for Na^+ and K^+, compared to bulk, as shown in Figure 3C. The interaction between both cations and the water in the remaining region in CNTs is extremely weak, while their remaining region in bulk is on average repulsive by 4−6 kJ mol^{-1} as shown in Figure 3D. Therefore, we speculate that the interaction between ions and the water molecules beyond 1 nm of ions should be so weak that it can be ignored in our analysis. Quite different from the situation for cations, E_1, E_2 and E_3 of Cl^- increase gradually to the bulk value with increasing CNT diameter. In addition, the interaction between Cl^- and water in the remaining region in bulk is attractive. We presume that these differences between cations and anions arise from difference in the characteristics of their hydration: Na^+ and K^+ are coordinated by the oxygen atoms of water molecules, while Cl^- is coordinated by the hydrogen atoms. When ions are confined in CNTs, the interaction between ions and water molecules in each of the hydration shells changes in a different way. We speculate that this is caused by the ionic hydration structures and specific water phase in CNTs, something that is explored in detail below.

It is important to note that the enhanced ion−water interaction energy seen in CNT(8,8) does not mean that it is more favorable to solvate cations in the CNT than in bulk, as this does not include other energetic interactions or entropy. In fact, the solvation free energy of Na^+ is 23.80 kJ mol^{-1} unfavorable in CNT(8,8) compared to bulk (see Supporting Information for simulation details.) This value is comparable to the free energy barrier for Na^+ passing across CNT(8,8) seen in previous simulations.[63,64]

Ionic Hydration Structures under CNT Confinement. Ion−oxygen radial distribution functions (RDFs) of Na^+, K^+ and Cl^- in CNTs and bulk solution have been analyzed and are displayed in Supporting Information Figure S1. We find that the nanoscale confinement of CNTs does not change the size of the ionic hydration shell, in accordance with previous results.[29,33] Figure 4 shows the coordination numbers of ions of their first shell (N_1), second shell (N_2) and the remaining region (N_3), which are calculated according to the numeric integration of the corresponding RDF profiles in Figure S1 in the Supporting Information. A great reduction of N_1 of these three ions is observed in CNT(6,6) and -(7,7), indicating severe dehydration, as their effective radii are smaller than the size of the first hydration shells. In CNT(6,6), Na^+ can disturb the single-file water chain more greatly than K^+ and Cl^-. Its

dx.doi.org/10.1021/jp4025206 | J. Phys. Chem. C 2013, 117, 11412−11420

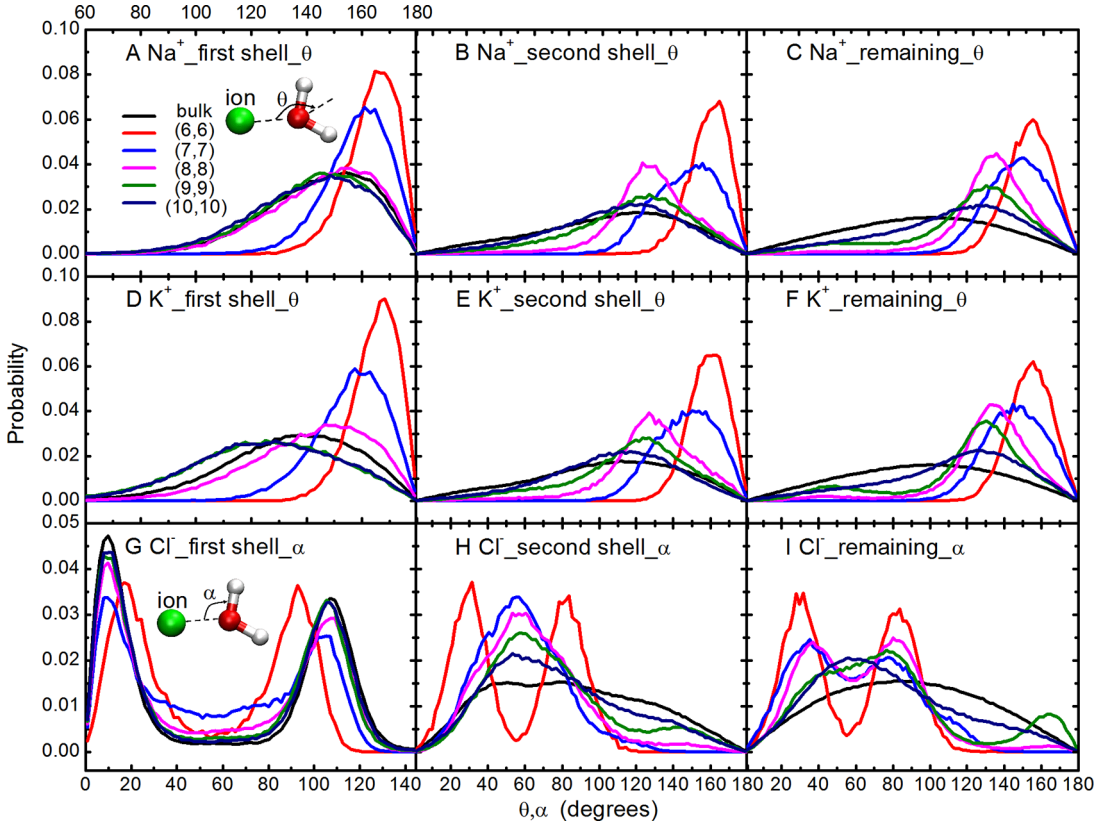

Figure 5. Probability distributions of the orientation angle θ and α of water molecules within the first shell and the second shell of ions and in the remaining region (that is beyond the second shell but within 1 nm of ions) in CNTs and bulk solution for Na^+ (A–C), K^+ (D–F) and Cl^- (G–I). The insets illustrate the definition of angles θ and α.

smaller size and stronger hydration ability make it even coordinated by 3 water molecules in the tube. Therefore, N_1 of Na^+ in CNT(6,6) is about 0.5 larger than that of K^+ and Cl^-, as shown in Figure 4A. In wider CNTs (8,8), (9,9) and (10,10), N_1 of Cl^- increases from 6.0 to 7.0, which is close to the bulk counterpart. Some anomalies occur in wide CNTs. The N_1 of K^+ in CNT(9,9) and -(10,10) is about 0.5 more than the bulk value. In addition, the N_1 of Na^+ in CNT(8,8) is larger than that in CNT(9,9), whose effective diameter is 0.135 nm larger than CNT(8,8). As shown in Figures 4A and 4B, the N_2 and N_3 of ions increase with the diameter of CNT, but are all less than the bulk counterparts, for the effective radii of all these CNTs are smaller than the size of the second hydration shell. Therefore, the second hydration shells and the remaining regions of ions are not intact when confined in these CNTs.

The orientation of water molecules around ions is another important factor in ionic hydration,[62,65,66] and Zhou et al.[62] proposed a parameter named hydration factor to investigate this orientation quantitatively. Here, to describe this orientation, θ was defined for Na^+ and K^+, and α for Cl^-. θ is the angle between the water dipole and the line joining the water oxygen to the ion, and α is the angle between O–H bond and the line joining the water oxygen to the ion, as illustrated in the insets of Figures 5A and 5G, respectively. When a cation is coordinated by a water molecule, the water oxygen atom points toward the ion and both hydrogen atoms point away. For an anion, one of the OH groups of a water molecule points toward it. Therefore, the optimal value of θ for cations is 180°, and the optimal value of α for anions is 0°. The actual value of θ and α usually deviates from these optimal values due to the competing interaction between water molecules in the hydration shells as shown in Figure 5. If the values of θ and α are closer to the optimal value, the hydration shell is more ordered and yields a more favorable ion–water interaction energy. Throughout this paper we refer to a hydration shell as being more "ordered" when the water dipoles are closer to that yielding optimum ion–water interaction, rather than using this to describe entropic factors. For Na^+ and K^+ in the bulk solution, the distribution curve of θ for the first shell presents a wide peak with the maximum located at around 150° as shown in Figures 5A and 5D, respectively. When confined in CNT(6,6) and -(7,7), the sharp peaks of the profiles are at 160°–180°. In CNT(8,8), the peak is shifted to slightly higher values than in bulk, while in CNT(9,9) and CNT(10,10) it is at slightly lower values than in bulk. Therefore, the first hydration shell of Na^+ becomes much more ordered than bulk in narrow CNTs and slightly less ordered in wide CNTs. As shown in Figure 5G, for Cl^- in the bulk solution, the distribution curve of α for its first shell presents two sharp peaks with the maximal located at around 10° and 110° respectively, indicating that one hydrogen atom of a water molecule points to Cl^- (corresponding to 10°) and the other points away (corresponding to 110°). Only in CNT(6,6), the two peaks are shifted to 20° and 90°, thus, the first hydration shell of Cl^- is much less ordered than the bulk one. In other CNTs, the peak positions almost do not change compared to bulk and the height of the peak has only to increase slightly to reach the bulk level. Therefore, the first hydration shell of Cl^- is only slightly less ordered in wider CNTs than in bulk.

dx.doi.org/10.1021/jp4025206 | J. Phys. Chem. C 2013, 117, 11412–11420

As the water molecules in the second shell and remaining region do not contact ions directly, the orientation of water molecules in these two regions is more significantly affected by the overall water structure in the CNT. As shown in Figure 6

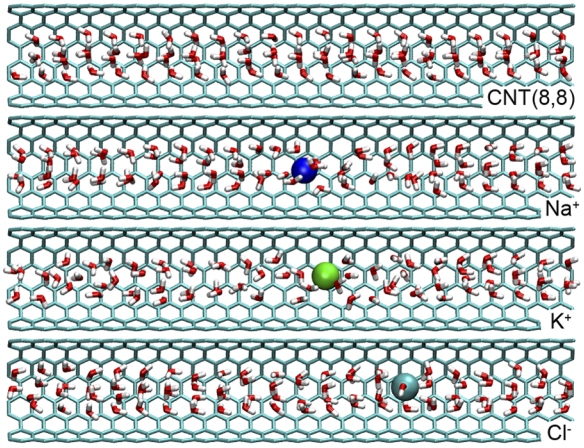

Figure 6. The structure and orientation of water in CNT(8,8), showing the changes that arise when ions are present.

and Figure S2 in the Supporting Information, when an ion is solvated in CNTs, the water structures and dipole orientation are changed. For Na^+ and K^+, the dipoles of water molecules in CNTs on the left side of the ion concertedly point leftward, and those of water molecules on the right side concertedly point rightward. For Cl^-, the opposite is the case. Such concertedness of water molecule orientations is caused by the hydrogen bonds connecting them. These changes lead to the enhancement in the interaction of cations with the second shells seen in Figure 3C. As shown in Figure 5B, 5C, 5E and 5F, for Na^+ and K^+ in CNT(6,6), the distribution curves of θ present a sharp peak with the maximum located at around 170°. The peaks slowly become wider and shift toward the bulk positions in the wider CNTs, indicating that the second and the remaining hydration shells of Na^+ and K^+ are more ordered in CNTs than their bulk counterparts, and become less ordered with increased CNT diameter. As for Cl^- in CNT(6,6), as depicted in Figures 5H and 5I, the distribution curves of α present two sharp peaks with the maxima located at around 30° and 80° respectively, which originates from the single-file water structure. From CNT(7,7) to CNT(10,10) and bulk, the probability of α falling in the range of 90°−180° increases, indicating that more hydrogen atoms point away from Cl^-. Hence, like the case of Na^+ and K^+, the order of second shell and remaining region of Cl^- is higher in narrow CNTs and decreases to bulk level with the increase of CNT diameter. On the whole, the water structures in CNTs make the second shell and remaining region of ions more ordered, meaning that they orient in a way that produces enhanced electrostatic interactions with the ion. We can find that all the hydration shells of Na^+ and K^+ in CNT(8,8) are more oriented to yield more favorable electrostatic interactions with the ions than the bulk counterparts.

The change of coordination number and hydration shell orientation can explain the anomalous ion−water interaction change for cations. When the hydration shell is more ordered, the average interaction between an ion and a single water molecule is stronger as shown in Figure S3 in the Supporting Information. If ions are coordinated by more water molecules with more favorable orientation, the interaction between ions and water will be stronger. The reduced interaction energy between cations and water molecules in their first shell (E_1) seen in CNT(6,6) and -(7,7) is caused by dehydration although the more ordered hydration shell partly compensates this effect. In CNT(9,9) and -(10,10), E_1 of Na^+ and K^+ is slightly weakened due to the less ordered hydration shell, despite the coordination number being close to or larger than bulk. In contrast, for Na^+ in CNT(8,8) first shell hydration number (N_1) and hydration shell orientation are both bulk-like; while for K^+ the obvious more optimal orientation of the first hydration shell perfectly compensates the slight decrease in N_1. Given that the interaction with the first shell is bulk-like, the magnitude of the total ion−water interaction energy for both cations in CNT(8,8) is greater than in bulk due to the more favorable orientation of the second hydration shell, which overcomes the fact that the coordination numbers in the second shell are less than in bulk. A similar enhanced ion−water interaction does not arise for Cl^- as both the hydration number and orientation in the first shell progress monotonically toward the bulk values as the CNT diameter increases.

The radial distribution of ions and water inside the CNT, as shown in Figures 7 and 8, can affect ionic hydration in CNTs. It

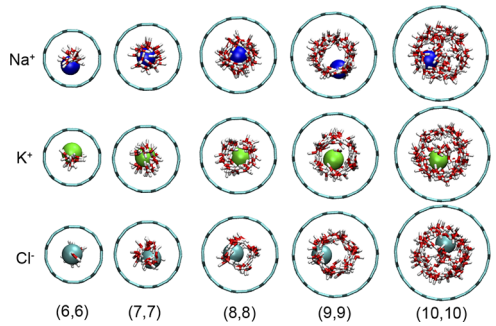

Figure 7. Cross-sectional views of the radial distribution of Na^+, K^+ and Cl^- in CNTs.

is found that the close-packed and ordered water molecules in CNT(8,8) perfectly coordinate Na^+ and K^+ at the tube axis, as depicted in Figure 8C, making the interaction of cations with the first hydration shell bulk-like. As shown in Figures 8D and 8E, in wider CNT(9,9) and -(10,10), K^+ prefers to reside near the tube central axis, far from the location of most of the water, which creates a loosely organized and less ordered first hydration shell. Na^+ prefers to stay off the tube axis, closer to the water layer than K^+, leading to the more ordered first hydration shell than K^+. These radial positions are energetically favorable for Na^+ and K^+, as evidenced by previous 2D free energy calculation results.[33,63] As shown in Figures 8A, 8B, 8C, 8D and 8E, in all the CNTs, the peak in the Cl^- distribution is always located about 0.1 nm closer to the tube axis than the peak of water oxygen atoms, as it has to be coordinated by the hydrogen atoms of water molecules. Cl^- is seen to often insert into the water columns in CNTs without much disruption, as shown in Figure 7. This phenomenon was also observed in boron nitride nanotubes.[67] We speculate that this is caused by the characteristics of anion hydration: Cl^- is coordinated by one hydrogen atom of a water molecule, which leaves another hydrogen atom free to form hydrogen bonds with other water molecules. In contrast, water molecules that coordinate cations cannot form hydrogen bonds through the oxygen, and the

dx.doi.org/10.1021/jp4025206 | J. Phys. Chem. C 2013, 117, 11412−11420

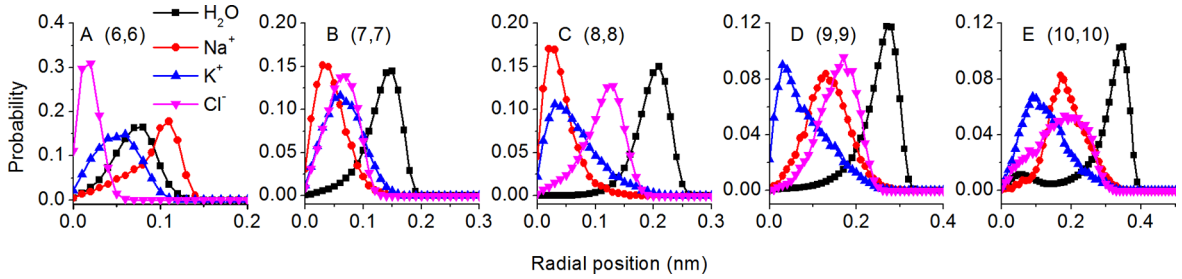

Figure 8. The radial distribution of Na^+, K^+, Cl^- and water molecules in different CNTs. (A) (6,6), (B) (7,7), (C) (8,8), (D) (9,9) and (E) (10,10). The radial position of the tube axis is 0.

orientation of both hydrogen atoms is changed profoundly by the ion, making it difficult for them to form hydrogen bonds. Thus, the disruption of anion hydration to water structures is much less than that of cations, as shown in Figure 7.

Effect of Hydrogen Bonds of Water on Ionic Hydration under CNT Confinement. When arranging water molecules around the ions, there is a direct competition between water−water interactions (i.e., hydrogen bonding) and ion−water interaction (i.e., ionic hydration), and the geometric constraint of CNTs (confinement) plays a role as well. The hydrogen bonds formed among the water molecules in the first hydration shells of Na^+, K^+ and Cl^- are analyzed, and the average number is plotted in Figure 9. In CNT(6,6), almost no

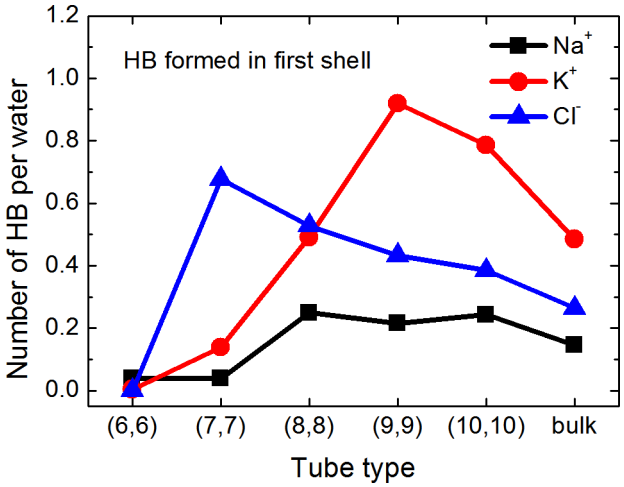

Figure 9. Average number of hydrogen bond (HB) per water formed between the water molecules in the first shell of Na^+, K^+ and Cl^- in CNTs and the bulk.

hydrogen bonds are formed among the water molecules in the first hydration shell due to the extreme confinement, therefore, the order of the first hydration shell is mainly determined by the ion−water electrostatic interaction and the confinement effect in this tube. For Cl^-, from CNT(7,7) to -(10,10), the average hydrogen bond per water formed in the hydration shell decreases gradually to the bulk level with the CNT diameter. This means that the orientation of water molecules in the first hydration shell around Cl^- is influenced more by water−water hydrogen bonds in the CNTs than is the case in bulk. Therefore, the first hydration shell order of Cl^- increases gradually to the bulk value, as shown in Figure 5G. For K^+ in CNT(9,9) and -(10,10), many more hydrogen bonds are formed than in bulk, and the water molecules in the first shell can be hydrogen bonded even to form a cage, which enwraps K^+ in its center. This means that the water−water interaction is so strong that it can surpass the relative weak interaction between K^+ and the first shell, making the shell less ordered. For Na^+ in CNT(8,8), -(9,9) and -(10,10), the average number of hydrogen bonds is closer to bulk than for K^+ and Cl^- due to stronger hydration of this ion.[61] As for the water molecules in the second shell and the remaining region of ions confined in CNTs, they lose at least 0.5 hydrogen bond on average, as shown in Figure S4 in the Supporting Information. Thus, the hydrogen bonds at longer distance are broken, which agrees well with the results of the recent X-ray diffraction study[39] of NaCl aqueous solution confined in CNTs.

CONCLUSIONS

Molecular dynamics simulations have been performed to study the hydration properties of Na^+, K^+ and Cl^- when confined in CNTs of different diameter. The results show that ice-like water structures are formed in CNT(8,8) and -(9,9), which can affect ionic hydration profoundly. For Na^+ and K^+, their interaction energy with the first hydration shell is greatly weakened in CNT(6,6) and -(7,7) due to severe dehydration in spite of more ordered hydration structures, and is slightly weakened in CNT(9,9) and -(10,10) due to the less optimally oriented hydration structures. However, the first hydration shells of both cations in CNT(8,8) are similar to the bulk counterparts, as the coordination numbers are close to or slightly less than the bulk values and their first hydration shells are well oriented. In all the CNTs, the interaction of Na^+ and K^+ with the second hydration shells is enhanced compared to bulk. This phenomenon is caused by the fact that water forms highly structured "ice-like" arrangements in the CNTs, which leaves the water with dipole orientations that favorably interact with Na^+ and K^+. As a consequence, the cation−water interaction is stronger in CNT(8,8) than in bulk. Nevertheless, this does not mean the hydration of Na^+ and K^+ in this tube is more favorable than in bulk as water−water and entropic changes also influence the total free energy change of the ion entering the CNT. In contrast, the interaction energies of Cl^- with all hydration shells are strengthened gradually to the bulk level with increasing CNT diameter. It seems that Cl^- can insert into the water columns in CNTs with minimal disruption, but Cl^- does not benefit from favorable water dipole orientations in the CNTs as do the cations. For Cl^-, the coordination number may be more important than hydration shell orientation in determining the ion−water interaction energy. In all the CNTs, hydrogen bonds formed among water molecules in the second shell and other longer range are weakened; while more hydrogen bonds can be formed within the first hydration shell in some CNTs, which makes the ion−water dipole orientation less optimal and reduces the ion−

dx.doi.org/10.1021/jp4025206 | J. Phys. Chem. C 2013, 117, 11412−11420

water interaction. These new findings improve our understanding of the hydration of ions in confined spaces and the effect that unique "ice-like" water structures present in CNTs can have on ionic hydration.

■ ASSOCIATED CONTENT

Supporting Information

Ion−oxygen radial distribution functions, water dipole orientations in CNTs, simulation details for ionic hydration free energy calculation, average interaction energy between an ion and a single water molecule, and hydrogen bonds formed in the hydration shells of ions. This material is available free of charge via the Internet at http://pubs.acs.org.

■ AUTHOR INFORMATION

Corresponding Author

*E-mail: jianzhou@scut.edu.cn; ben.corry@anu.edu.au.

Notes

The authors declare no competing financial interest.

■ ACKNOWLEDGMENTS

This work was supported by the National Key Basic Research Program of China (No. 2013CB733501), Program for New Century Excellent Talents in University (NCET-07-0313), National Natural Science Foundation of China (No. 20876052) and Guangdong Science Foundation (No. S2011010002078). The computational resources for this project are provided by the National Supercomputing Centre in Shenzhen (China) and additional computer time from the National Computational Infrastructure (NCI) National Facility (Australia). Z.H. thanks the China Scholarship Council for support.

■ REFERENCES

(1) Holt, J. K.; Park, H. G.; Wang, Y. M.; Stadermann, M.; Artyukhin, A. B.; Grigoropoulos, C. P.; Noy, A.; Bakajin, O. Fast Mass Transport through Sub-2-nanometer Carbon Nanotubes. *Science* **2006**, *312*, 1034−1037.

(2) Majumder, M.; Chopra, N.; Andrews, R.; Hinds, B. J. Nanoscale Hydrodynamics: Enhanced Flow in Carbon Nanotubes. *Nature* **2005**, *438*, 44−44.

(3) Ghosh, S.; Sood, A. K.; Kumar, N. Carbon Nanotube Flow Sensors. *Science* **2003**, *299*, 1042−1044.

(4) Regan, B. C.; Aloni, S.; Ritchie, R. O.; Dahmen, U.; Zettl, A. Carbon Nanotubes as Nanoscale Mass Conveyors. *Nature* **2004**, *428*, 924−927.

(5) Lee, C. Y.; Choi, W.; Han, J. H.; Strano, M. S. Coherence Resonance in a Single-Walled Carbon Nanotube Ion Channel. *Science* **2010**, *329*, 1320−1324.

(6) Fornasiero, F.; Park, H. G.; Holt, J. K.; Stadermann, M.; Grigoropoulos, C. P.; Noy, A.; Bakajin, O. Ion Exclusion by Sub-2-nm Carbon Nanotube Pores. *Proc. Natl. Acad. Sci. U.S.A.* **2008**, *105*, 17250−17255.

(7) Corry, B. Designing Carbon Nanotube Membranes for Efficient Water Desalination. *J. Phys. Chem. B* **2008**, *112*, 1427−1434.

(8) Jia, Y. X.; Li, H. L.; Wang, M.; Wu, L. Y.; Hu, Y. D. Carbon Nanotube: Possible Candidate for Forward Osmosis. *Sep. Purif. Technol.* **2010**, *75*, 55−60.

(9) Corry, B. Water and Ion Transport through Functionalised Carbon Nanotubes: Implications for Desalination Technology. *Energy Environ. Sci.* **2011**, *4*, 751−759.

(10) Hilder, T. A.; Gordon, D.; Chung, S.-H. Computational Modeling of Transport in Synthetic Nanotubes. *Nanomed. Nanotechnol. Biol. Med.* **2011**, *7*, 702−709.

(11) Garcia-Fandino, R.; Sansom, M. S. P. Designing Biomimetic Pores based on Carbon Nanotubes. *Proc. Natl. Acad. Sci. U.S.A.* **2012**, *109*, 6939−6944.

(12) Gong, X. J.; Li, J. C.; Xu, K.; Wang, J. F.; Yang, H. A Controllable Molecular Sieve for Na^+ and K^+ Ions. *J. Am. Chem. Soc.* **2010**, *132*, 1873−1877.

(13) Zhao, W. H.; Shang, B.; Du, S. P.; Yuan, L. F.; Yang, J.; Zeng, X. C. Highly Selective Adsorption of Methanol in Carbon Nanotubes Immersed in Methanol-water Solution. *J. Chem. Phys.* **2012**, *137*, 034501.

(14) Shao, Q.; Huang, L. L.; Zhou, J.; Lu, L. H.; Zhang, L. Z.; Lu, X. H.; Jiang, S. Y.; Gubbins, K. E.; Zhu, Y. D.; Shen, W. F. Molecular dynamics study on diameter effect in structure of ethanol molecules confined in single-walled carbon nanotubes. *J. Phys. Chem. C* **2007**, *111*, 15677−15685.

(15) Noskov, S. Y.; Roux, B. Importance of Hydration and Dynamics on the Selectivity of the KcsA and NaK Channels. *J. Gen. Physiol.* **2007**, *129*, 135−143.

(16) Shi, N.; Ye, S.; Alam, A.; Chen, L. P.; Jiang, Y. X. Atomic Structure of a Na^+- and K^+-Conducting Channel. *Nature* **2006**, *440*, 570−574.

(17) Corry, B.; Thomas, M. Mechanism of Ion Permeation and Selectivity in a Voltage Gated Sodium Channel. *J. Am. Chem. Soc.* **2012**, *134*, 1840−1846.

(18) Beckstein, O.; Sansom, M. S. P. A Hydrophobic Gate in an Ion Channel: the Closed State of the Nicotinic Acetylcholine Receptor. *Phys. Biol.* **2006**, *3*, 147−159.

(19) Ohba, T.; Kojima, N.; Kanoh, H.; Kaneko, K. Unique Hydrogen-Bonded Structure of Water around Ca Ions Confined in Carbon Slit Pores. *J. Phys. Chem. C* **2009**, *113*, 12622−12624.

(20) Argyris, D.; Cole, D. R.; Striolo, A. Ion-Specific Effects under Confinement: The Role of Interfacial Water. *ACS Nano* **2010**, *4*, 2035−2042.

(21) Zhu, Y. D.; Zhou, J.; Lu, X. H.; Guo, X. J.; Lu, L. H. Molecular Simulations on Nanoconfined Water Molecule Behaviors for Nanoporous Material Applications. *Microfluid. Nanofluid.* **2013**, DOI: 10.1007/s10404-013-1143-7.

(22) Feng, H. J.; Zhou, J.; Lu, X. H. Molecular Dynamics Simulations on the Interfacial Structures of Electrolyte Solutions. *Acta Chim. Sinica* **2009**, *67*, 2407−2412.

(23) Feng, H. J.; Zhou, J.; Lu, X. H.; Fichthorn, K. A. Molecular Dynamics Simulations of the Interfacial Structure of Alkali Metal Fluoride Solutions. *J. Chem. Phys.* **2010**, *133*, 061103.

(24) Phillips, K. A.; Palmer, J. C.; Gubbins, K. E. Analysis of the Solvation Structure of Rubidium Bromide under Nanoconfinement. *Mol. Simul.* **2012**, *38*, 1209−1220.

(25) Leng, Y. S.; Cummings, P. T. Shear Dynamics of Hydration Layers. *J. Chem. Phys.* **2006**, *125*, 104701.

(26) Chialvo, A. A.; Cummings, P. T. Aqua Ions-Graphene Interfacial and Confinement Behavior: Insights from Isobaric-Isothermal Molecular Dynamics. *J. Phys. Chem. A* **2011**, *115*, 5918−5927.

(27) Nicholson, D.; Quirke, N. Ion Pairing in Confined Electrolytes. *Mol. Simul.* **2003**, *29*, 287−290.

(28) Malani, A.; Ayappa, K. G.; Murad, S. Effect of Confinement on the Hydration and Solubility of NaCl in Water. *Chem. Phys. Lett.* **2006**, *431*, 88−93.

(29) Liu, H. M.; Murad, S.; Jameson, C. J. Ion Permeation Dynamics in Carbon Nanotubes. *J. Chem. Phys.* **2006**, *125*, 084713.

(30) Shao, Q.; Zhou, J.; Lu, L. H.; Lu, X. H.; Zhu, Y. D.; Jiang, S. Y. Anomalous Hydration Shell Order of Na^+ and K^+ inside Carbon Nanotubes. *Nano Lett.* **2009**, *9*, 989−994.

(31) Cazade, P. A.; Dweik, J.; Coasne, B.; Henn, F.; Palmeri, J. Molecular Simulation of Ion-Specific Effects in Confined Electrolyte Solutions Using Polarizable Forcefields. *J. Phys. Chem. C* **2010**, *114*, 12245−12257.

(32) Kulik, H. J.; Schwegler, E.; Galli, G. Probing the Structure of Salt Water under Confinement with First-Principles Molecular Dynamics and Theoretical X-ray Absorption Spectroscopy. *J. Phys. Chem. Lett.* **2012**, *3*, 2653−2658.

(33) Peter, C.; Hummer, G. Ion Transport through Membrane-spanning Nanopores Studied by Molecular Dynamics Simulations and Continuum Electrostatics Calculations. *Biophys. J* . **2005**, *89*, 2222−2234.
(34) Shao, Q.; Huang, L. L.; Zhou, J.; Lu, L. H.; Zhang, L. Z.; Lu, X. H.; Jiang, S. Y.; Gubbins, K. E.; Shen, W. F. Molecular Simulation Study of Temperature Effect on Ionic Hydration in Carbon Nanotubes. *Phys. Chem. Chem. Phys.* **2008**, *10*, 1896−1906.
(35) Ohkubo, T.; Konishi, T.; Hattori, Y.; Kanoh, H.; Fujikawa, T.; Kaneko, K. Restricted Hydration Structures of Rb and Br Ions Confined in Slit-shaped Carbon Nanospace. *J. Am. Chem. Soc.* **2002**, *124*, 11860−11861.
(36) Ohkubo, T.; Nishi, M.; Kuroda, Y. Actual Structure of Dissolved Zinc Ion Restricted in Less Than 1 Nanometer Micropores of Carbon. *J. Phys. Chem. C* **2011**, *115*, 14954−14959.
(37) Levi, M. D.; Sigalov, S.; Salitra, G.; Elazari, R.; Aurbach, D. Assessing the Solvation Numbers of Electrolytic Ions Confined in Carbon Nanopores under Dynamic Charging Conditions. *J. Phys. Chem. Lett.* **2011**, *2*, 120−124.
(38) Nishi, M.; Ohkubo, T.; Tsurusaki, K.; Itadani, A.; Ahmmad, B.; Urita, K.; Moriguchi, I.; Kittaka, S.; Kuroda, Y. Highly Compressed Nanosolution Restricted in Cylindrical Carbon Nanospaces. *Nanoscale* **2013**, *5*, 2080−2088.
(39) Ohba, T.; Hata, K.; Kanoh, H. Significant Hydration Shell Formation Instead of Hydrogen Bonds in Nanoconfined Aqueous Electrolyte Solutions. *J. Am. Chem. Soc.* **2012**, *134*, 17850−17853.
(40) Marcus, Y. Effect of Ions on the Structure of Water: Structure Making and Breaking. *Chem. Rev.* **2009**, *109*, 1346−1370.
(41) Koga, K.; Gao, G. T.; Tanaka, H.; Zeng, X. C. Formation of Ordered Ice Nanotubes inside Carbon Nanotubes. *Nature* **2001**, *412*, 802−805.
(42) Mashl, R. J.; Joseph, S.; Aluru, N. R.; Jakobsson, E. Anomalously Immobilized Water: A New Water Phase Induced by Confinement in Nanotubes. *Nano Lett.* **2003**, *3*, 589−592.
(43) Byl, O.; Liu, J. C.; Wang, Y.; Yim, W. L.; Johnson, J. K.; Yates, J. T. Unusual Hydrogen Bonding in Water-filled Carbon Nanotubes. *J. Am. Chem. Soc.* **2006**, *128*, 12090−12097.
(44) Hummer, G.; Rasaiah, J. C.; Noworyta, J. P. Water Conduction through the Hydrophobic Channel of a Carbon Nanotube. *Nature* **2001**, *414*, 188−190.
(45) Berendsen, H. J. C.; Grigera, J. R.; Straatsma, T. P. The Missing Term in Effective Pair Potentials. *J. Phys. Chem.* **1987**, *91*, 6269−6271.
(46) Darden, T.; York, D.; Pedersen, L. Particle Mesh Ewald: An N·log(N) Method for Ewald Sums in Large Systems. *J. Chem. Phys.* **1993**, *98*, 10089−10092.
(47) Miyamoto, S.; Kollman, P. A. Settle: An Analytical Version of the SHAKE and RATTLE Algorithm for Rigid Water Models. *J. Comput. Chem.* **1992**, *13*, 952−962.
(48) Nose, S. A Molecular Dynamics Method for Simulations in the Canonical Ensemble. *Mol. Phys.* **1984**, *52*, 255−268.
(49) Hess, B.; Kutzner, C.; van der Spoel, D.; Lindahl, E. GROMACS 4: Algorithms for Highly Efficient, Load-Balanced, and Scalable Molecular Simulation. *J. Chem. Theory Comput.* **2008**, *4*, 435−447.
(50) Luo, C. F.; Fa, W.; Zhou, J.; Dong, J. M.; Zeng, X. C. Ferroelectric ordering in ice nanotubes confined in carbon nanotubes. *Nano Lett.* **2008**, *8*, 2607−2612.
(51) Mikami, F.; Matsuda, K.; Kataura, H.; Maniwa, Y. Dielectric Properties of Water inside Single-Walled Carbon Nanotubes. *ACS Nano* **2009**, *3*, 1279−1287.
(52) Soper, A. K.; Bruni, F.; Ricci, M. A. Site-site Pair Correlation Functions of Water From 25 to 400 °C: Revised Analysis of New and Old Diffraction Data. *J. Chem. Phys.* **1997**, *106*, 247−254.
(53) Wang, J.; Zhu, Y.; Zhou, J.; Lu, X. H. Diameter and Helicity Effects on Static Properties of Water Molecules Confined in Carbon Nanotubes. *Phys. Chem. Chem. Phys.* **2004**, *6*, 829−835.
(54) Zhang, H. W.; Ye, H. F.; Zheng, Y. G.; Zhang, Z. Q. Prediction of the Viscosity of Water Confined in Carbon Nanotubes. *Microfluid. Nanofluid.* **2011**, *10*, 403−414.
(55) Bai, J. E.; Wang, J.; Zeng, X. C. Multiwalled Ice Helixes and Ice Nanotubes. *Proc. Natl. Acad. Sci. U.S.A.* **2006**, *103*, 19664−19667.
(56) Kyakuno, H.; Matsuda, K.; Yahiro, H.; Inami, Y.; Fukuoka, T.; Miyata, Y.; Yanagi, K.; Maniwa, Y.; Kataura, H.; Saito, T.; et al. Confined Water inside Single-walled Carbon Nanotubes: Global Phase Diagram and Effect of Finite Length. *J. Chem. Phys.* **2011**, *134*, 244501.
(57) Ohba, T.; Taira, S.; Hata, K.; Kaneko, K.; Kanoh, H. Predominant Nanoice Growth in Single-walled Carbon Nanotubes by Water-vapor Loading. *RSC Advances* **2012**, *2*, 3634−3637.
(58) Jazdzewska, M.; Sliwinska-Bartkowiak, M. M.; Beskrovnyy, A. I.; Vasilovskiy, S. G.; Ting, S. W.; Chan, K. Y.; Huang, L. L.; Gubbins, K. E. Novel Ice Structures in Carbon Nanopores: Pressure Enhancement Effect of Confinement. *Phys. Chem. Chem. Phys.* **2011**, *13*, 9008−9013.
(59) Ye, H. F.; Zhang, H. W.; Zheng, Y. G.; Zhang, Z. Q. Nanoconfinement Induced Anomalous Water Diffusion inside Carbon Nanotubes. *Microfluid. Nanofluid.* **2011**, *10*, 1359−1364.
(60) Ohba, T.; Kanoh, H. Energetic contribution to hydration shells in one-dimensional aqueous electrolyte solution by anomalous hydrogen bonds. *Phys. Chem. Chem. Phys.* **2013**, *15*, 5658−5663.
(61) Lee, S. H.; Rasaiah, J. C. Molecular Dynamics Simulation of Ion Mobility. 2. Alkali Metal and Halide Ions Using the SPC/E Model for Water at 25 °C. *J. Phys. Chem.* **1996**, *100*, 1420−1425.
(62) Zhou, J.; Lu, X. H.; Wang, Y. R.; Shi, J. Molecular Dynamics Study on Ionic Hydration. *Fluid Phase Equilib.* **2002**, *194*, 257−270.
(63) Song, C.; Corry, B. Intrinsic Ion Selectivity of Narrow Hydrophobic Pores. *J. Phys. Chem. B* **2009**, *113*, 7642−7649.
(64) He, Z. J.; Zhou, J. Steered Molecular Dynamics Simulations of Ions Traversing Through Carbon Nanotubes. *Acta Chim. Sinica* **2011**, *69*, 2901−2907.
(65) Rasaiah, J. C.; Noworyta, J. P.; Koneshan, S. Structure of Aqueous Solutions of Ions and Neutral Solutes at Infinite Dilution at a Supercritical Temperature of 683 K. *J. Am. Chem. Soc.* **2000**, *122*, 11182−11193.
(66) Zhu, Y. D.; Guo, X. J.; Shao, Q.; Wei, M. J.; Wu, X. M.; Lu, L. H.; Lu, X. H. Molecular Simulation Study of the Effect of Inner Wall Modified Groups on Ionic Hydration Confined in Carbon Nanotube. *Fluid Phase Equilib.* **2010**, *297*, 215−220.
(67) Hilder, T. A.; Gordon, D.; Chung, S. H. Boron Nitride Nanotubes Selectively Permeable to Cations or Anions. *Small* **2009**, *5*, 2870−2875.